

## Germanium diffusion mechanisms in silicon from first principles

Damien Caliste, Pascal Pochet, Thierry Deutsch, and Frédéric Lançon

*Département de Recherche Fondamentale sur la Matière Condensée, SP2M/L\_Sim, CEA/Grenoble, F-38054, Grenoble Cedex 9, France*

(Received 2 October 2006; revised manuscript received 21 December 2006; published 8 March 2007)

We present an extensive numerical study of the basic mechanisms that describe germanium diffusion in silicon mediated by point defects. This diffusion can be created by vacancies, interstitial atoms, or fourfold coordinated defects. All energies and elementary barriers have been precisely determined by *ab initio* calculations. The results for vacancies are compared with recently published values. The complex interstitial landscape is systematized and the key role of the hexagonal location is stressed as a halfway stable state between two, more stable, dumbbell [110] states. Finally, the mechanism of a concerted exchange linking two fourfold coordinated defects is fully calculated. Its activation energy is higher than for interstitial or vacancy mediated movements.

DOI: [10.1103/PhysRevB.75.125203](https://doi.org/10.1103/PhysRevB.75.125203)

PACS number(s): 66.30.Jt, 31.15.Ew, 61.72.Ji

### I. INTRODUCTION

Germanium is a technologically important compound in alloys used in the microelectronic industry. Transistors using a channel made of SiGe are more common, and several technical studies are conducted in this field (see Ref. 1 for a recent review). To improve the efficiency of such devices, it is important to control the diffusion of germanium through the silicon. Another common usage of germanium is to consider it as a siliconlike atom for diffusion, but there is no theoretical support for this hypothesis.

Since the early work of McVay and DuCharme,<sup>2</sup> several experimental studies<sup>3–5</sup> have been carried out to measure diffusivity values for germanium in SiGe alloys with varying concentration of germanium. These experiments reveal that activation energy ( $E_a$ ) is dependent on germanium concentration. As the concentration varies, a change in the mechanism responsible for germanium diffusion can explain the variation of  $E_a$ . There is a general agreement that vacancy mechanism occurs in a germanium-rich alloy (over 65%). A decade ago, Fahey *et al.*<sup>6</sup> experimentally demonstrated that both vacancies and interstitials activate the diffusion at a low concentration (lower than 35%). Different research groups (see Refs. 7–9) have simulated stable defects made of silicon or germanium, but their migrations have never been studied before, especially for interstitial-mediated movements.

In this article, we analyze, through numerical simulations, germanium diffusion in silicon crystals at low Ge concentrations. Since different point defects, including interstitials, vacancies, and fourfold coordinated defects, may play a role in atomic diffusion, the aims of this article are to list all stable defects of low energy where a Ge atom is involved and to give the elementary mechanisms of their migration. In many experimental conditions, the important concentration of germanium will create Ge-Ge pairs, and charge states will be present in certain conditions.<sup>10</sup> But, in this article, we only focus on isolated germanium, featuring a diluted limit without the effect of charge. This is a mandatory step to dealing with germanium atomic diffusion in silicon.

In the first part of the article, we briefly expose the computational methods and their parameters. In the second part, we concentrate on interstitial defects, giving values for their

formation energies and explaining which movements could appear. Then, we describe and analyze the concerted mechanism and the vacancy-assisted movements. Finally, we discuss the mutual implications of these mechanisms on diffusion.

### II. NUMERICAL DETAILS

We compute formation energies through *ab initio* calculations within the framework of the density-functional theory, using a plane wave method, with the code CPMD v3.8.<sup>11</sup> Our calculations are based on the local density approximation (LDA) with the Goedecker-Teter-Hutter pseudopotentials.<sup>12</sup> The LDA and the generalized gradient approximations give fairly different results in silicon,<sup>13</sup> but the experimental available data are not precise enough to validate either one or the other approximation. We therefore choose the LDA for our calculations since it is a long established approximation. The supercell consists in a box containing Si-crystal sites. One germanium atom is placed on a substitutional or an interstitial site. The box volume is fixed with a Si-Si bond distance of 2.35 Å. Atomic positions are relaxed until all forces become smaller than  $2.57 \times 10^{-2}$  eV/Å (i.e.,  $5 \times 10^{-4}$  hartree/bohr).

The formation energies are defined by  $E_f = E_{total} - N_{Si}\mu_{Si} - N_{Ge}\mu_{Ge}$ , where  $N_{Si}$  and  $N_{Ge}$  are the number of silicon and germanium atoms in a box whose energy is  $E_{total}$ . The energy of one single silicon atom in a perfect crystal defines  $\mu_{Si}$ , the chemical potential of silicon. The energy of one substitutional germanium atom in pure silicon is taken as the chemical potential for germanium ( $\mu_{Ge}$ ). The energy reference for all the following results are then a bulk system of silicon with one substitutional germanium.

The convergence of the *ab initio* calculations was checked with respect to the cutoff energy. We have conducted a cutoff study in supercells of 64 silicon sites plus a mixed SiGe dumbbell [110] and a  $2 \times 2 \times 2$  Monkhorst-Pack mesh.<sup>14</sup> We tested the cutoff range from 15 to 45 Ry. We choose 25 Ry for all further calculations since it gives a formation energy for the given system of only 0.9% higher than the one computed at 45 Ry.

A good integration of the Brillouin zone is necessary to give accurate values of formation energies and barriers. We

TABLE I. Formation energies of a mixed dumbbell and a mixed concerted defect, convergence study. Empty boxes correspond to systems not calculated (mostly for computational cost). FFCD stands for fourfold coordinated defect as defined by Goedecker *et al.* (Ref. 13).

Mixed dumbbell [110]	64 atoms	216 atoms	512 atoms
$1 \times 1 \times 1$	1.94 eV	2.82 eV	3.05 eV
$2 \times 2 \times 2$	3.13 eV	3.16 eV	
$3 \times 3 \times 3$	3.22 eV		
$4 \times 4 \times 4$	3.23 eV		
Mixed FFCD	64 atoms	216 atoms	512 atoms
$1 \times 1 \times 1$		2.35 eV	
$2 \times 2 \times 2$	2.83 eV	2.62 eV	
$3 \times 3 \times 3$	2.84 eV		

thus studied the influence of the number of elementary unit cells included in the supercell and of the sampling resolution in  $k$  space for all the defects that will be presented later in this article. To sum up this study, we detail in Table I the results for the mixed dumbbell [110] and the fourfold coordinated defect (FFCD) initially proposed by Goedecker *et al.*<sup>13</sup> It shows that  $k$  points are more important than the interaction between a defect and its replicas in the image boxes for the interstitial defects. Calculating energies in 64-site supercells with a  $2 \times 2 \times 2$   $k$  point sampling is the minimum requirement to have reliable values when interstitials are involved. In the following paragraphs, 216-site  $2 \times 2 \times 2$  boxes are used with interstitials to even lower the effect of interaction (still equal to 0.06 eV in a 64-site  $3 \times 3 \times 3$  system). The conclusion for the FFCD is quite different since a 216-site  $2 \times 2 \times 2$  system is the minimum requirement to correctly estimate the formation energy. This result is valid both in Si and SiGe, and it explains the discrepancies between the work of Goedecker *et al.*<sup>13</sup> and Al-Mushadani and Needs.<sup>15</sup> Indeed, Goedecker *et al.* had no size effect but a too limited  $k$  point sampling (reduced to  $\Gamma$  point only), whereas the opposite occurs in the calculations of Al-Mushadani and Needs. Concerning this issue of  $k$  point sampling versus box size for silicon vacancies, an extensive study can be found in the article of Probert and Payne,<sup>16</sup> and we consider it to be valid for a silicon system with one germanium, which means that boxes with 216 sites are of minimum size to avoid interactions between the vacancy and its replicas.

To describe diffusion, the minimum-energy paths between two given stable configurations have to be identified. To do this, we use the nudged elastic band (NEB) method<sup>17,18</sup> as implemented by Sbraccia.<sup>19</sup> Eight intermediate configurations (replicas) were chosen between two stable configurations. The forces in each replica were computed using CPMD (in boxes containing 64 sites at  $\Gamma$  point). The stop criterion is fixed to  $5.0 \times 10^{-2}$  eV/Å. Then to reach the saddle point, the replica with the highest energy after a NEB calculation is optimized with a DIIS (Ref. 20) algorithm and better *ab initio* convergence parameters: up to 216 sites and a  $2 \times 2 \times 2$   $k$  point mesh. The DIIS method is known to relax

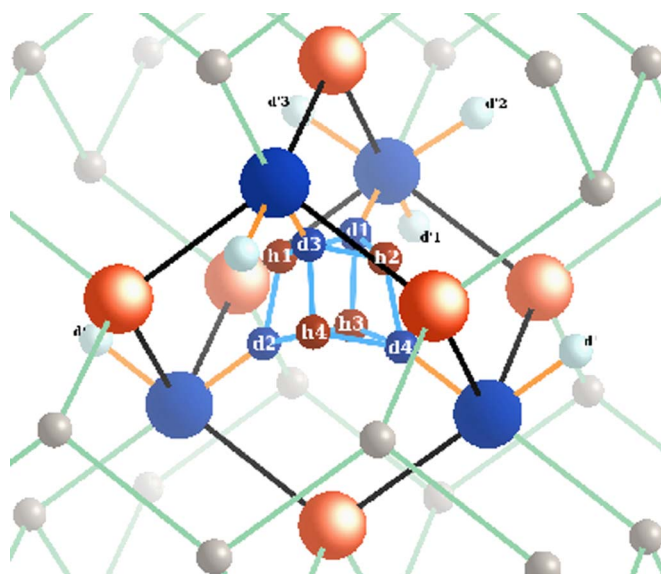


FIG. 1. (Color online) Representation of interstitial sites in the silicon lattice. Spheres labeled with letters stand for interstitial site, whereas other spheres are substitutional sites.  $d$ -type sites stand for dumbbell along [110] axis and are labeled with a “ $d$ ” letter;  $h$ -type sites represent hexagonal interstitials and are labeled with an “ $h$ .” Spheres labeled with prime letters do not belong to the represented ten-atom shape but are drawn, since they are used by [110] dumbbells. The pyramid is constituted of the four big blue (mat gray) spheres and all big spheres stand for the ten-atom shape.

toward a saddle point when the initial configuration is close enough to it. All saddle point configurations presented in this article have been computed through DIIS with convergence parameters identical to those used to find stable positions. Errors on barriers are thus similar to those of stable states.

### III. INTERSTITIAL DIFFUSION

We will now describe how the diffusion can be explained by interstitial migration. A convenient way to look at interstitials is to consider the tetrahedron formed by the second nearest neighbors (referred to as pyramid henceforth), as depicted in Fig. 1. Such a pyramid contains both hexagonal and dumbbell [110] interstitial sites. The tetrahedral site in Si (not represented) is positioned at the center of the pyramid. The pyramid can be extended to a ten-atom group by adding the six closest atoms (forming an octahedron). This new volume, with ten vertices, contains exactly the same interstitials as the pyramid and has the property of providing tiling for silicon lattice. It ensures that all mentioned interstitial sites will be described with the help of this pyramid.

The tested interstitial defects are commonly found in pure silicon. They include the hexagonal interstitial, the dumbbell geometry along [110] direction, and the tetrahedral interstitial. All three of them have been studied in pure silicon through first-principles calculations (see, e.g., Bar-Yam and Joannopoulos,<sup>21</sup> Blöchl *et al.*,<sup>22</sup> and Needs<sup>23</sup>). In our calculations, a silicon atom has been substituted by a germanium atom.

We label  $\text{Si}^H$  and  $\text{Si}^T$ , respectively, the hexagonal and tetrahedral defects when a silicon occupies the interstitial site.

TABLE II. Formation energies (in eV, calculated in a  $216$  site  $2 \times 2 \times 2$  system) for different defects in silicon with one germanium (first column). The second column gives the formation energies of equivalent defects in pure silicon. It highlights the small stabilizing effect of  $D^{110}$  in SiGe, since this column corresponds also to the energy of a Si interstitial and a Ge substitutional infinitely separated.

	SiGe	Si
Dumbbell ( $D^{110}$ )	3.16	3.22
Hexagonal	3.33 ( $\text{Si}^H$ )	3.25
	3.45 ( $\text{Ge}^H$ )	
Tetrahedral	Unstable (both $\text{Si}^T$ and $\text{Ge}^T$ )	Unstable
Vacancy	3.63	3.81
FFCD	2.62	2.59

In these configurations, the germanium is in a substitutional position and is one of the first neighbors of the defect. Defects labeled  $\text{Ge}^H$  and  $\text{Ge}^T$  are similar to the previous defects except that the germanium is now at the interstitial location. The final presented interstitial defect is a mixed SiGe dumbbell defect along  $[110]$  (labeled  $D^{110}$ ). Other interstitial defects (such as dumbbells along  $[001]$  or extended defects<sup>24</sup>) are not studied here because of their high formation energy.

The hexagonal defects are *displaced hexagonals* as reported for pure silicon in Ref. 15, i.e., there are two degenerated positions for the hexagonal interstitial on either side of the hexagonal ring of first neighbors. Thus, in the case of  $\text{Si}^H$  defect, all positions on the six sites of the surrounding ring are not equivalent. There are two possibilities where the substitutional Ge is  $2.47$  or  $2.44$  Å of the interstitial Si. Nevertheless, our calculations have shown that the energies of these two configurations are only separated by less than  $0.01$  eV (calculated in supercells of  $216$  sites at  $\Gamma$  point). Thus, the same name  $\text{Si}^H$  will refer to both kinds of configurations.

The computed formation energies of all these interstitial defects are shown in the first part of Table II. Tetrahedral defects have been found to be unstable since  $\text{Ge}^T$  and  $\text{Si}^T$ , respectively, relaxed to  $\text{Ge}^H$  and  $\text{Si}^H$ .

The mixed  $D^{110}$  is the most stable interstitial defect that includes one germanium atom. Its energy is close to that of an interstitial silicon defect and a separated substitutional germanium. We conclude that if interstitials are present in silicon with low germanium concentrations, these interstitials are mainly silicon interstitials (hexagonal or  $D^{110}$ ) and mixed SiGe  $D^{110}$  interstitials. Other defects ( $\text{Si}^H$  and  $\text{Ge}^H$ ) are less stable but with small energy differences. These results are in good agreement with those presented by Wang *et al.*,<sup>9</sup> except for  $\text{Ge}^T$ . According to Wang *et al.*,<sup>9</sup>  $\text{Ge}^T$  is a stable defect, whereas our calculations show unstable behavior. This mismatch may be related to imposing or not imposing symmetry during the calculations: we found a stable tetrahedral defect when symmetry constraints were imposed (with a similar formation energy compared to that of Wang *et al.*); on the contrary, when the symmetry is removed, the tetrahedral defect relaxed to a hexagonal defect.

Up to now, we have presented the most stable interstitial defects. The next step is to describe all elementary movements that link them together. Thus a comprehensive study was conducted using NEB calculations. The key result of this study is that all interstitial movements involving a germanium atom can be broken down into three elementary movements labeled  $dh$  movement,  $hh$  movement, and  $b$  movement. During a  $dh$  movement, a dumbbell  $[110]$  is moved into a hexagonal interstitial [see Fig. 2(a)]. An  $hh$  movement describes the possibility of linking two hexagonal interstitials within a pyramid [see Fig. 2(b)]. Finally, at the boundary of two pyramids, a  $b$  movement links two degenerated *displaced hexagonal* configurations through a low-energy barrier [see Fig. 2(c)]. It should be noted that no direct jump path connects the most stable sites (namely,  $D^{110}$  positions).

The germanium diffusion throughout the silicon lattice requires linking these previous elementary movements in two steps: a jump between different pyramids and a diffusion inside each pyramid itself. The former step is achieved by the use of  $b$  movement or  $dh$  movements with  $\text{Si}^H$  as the hexagonal state. We can illustrate this last movement in Fig. 1 by setting a silicon on the  $d1$  site and a germanium on the  $d'1$  site. The silicon moves first to the  $h2$  (or  $h1$ ) site and the germanium becomes substitutional. Then the silicon returns to the  $d1$  site and the germanium goes to the  $d'3$  (or  $d'2$ ) site, creating a  $D^{110}$  in another pyramid. The latter step of the diffusion (moving inside a pyramid) is achieved by one or several  $hh$  movements (involving  $\text{Ge}^H$ ) or  $dh$  movements (with  $\text{Ge}^H$  as hexagonal state).

The energetic costs of such movements are summarized in Table III. Similar behaviors for  $dh$  movements and  $hh$  movements have already been studied by Needs<sup>23</sup> in pure silicon. Such a qualitative agreement between Si-based and Ge-based interstitial diffusion mechanisms is an argument in favor of the proposal to use germanium as a tracer for silicon self-diffusion, e.g., Fahey *et al.*<sup>6</sup> The quantitative comparison with Needs results is more complex due to different convergence parameters and relaxation algorithms. In a first glance, the barriers are quite different: Needs reports them to be  $0.15$  eV for  $dh$  movements in silicon, whereas we found  $0.37$  and  $0.44$  eV, respectively, for  $\text{Si}^H$  and  $\text{Ge}^H$ . But this discrepancy is due, in a part, to the fact that  $D^{110}$  defects are lower in energy in SiGe. Removing this effect, by considering reverse barriers (going from a hexagonal defect to a dumbbell one), reduces the figures to  $0.20$  and  $0.15$  eV, respectively, for  $\text{Si}^H$  and  $\text{Ge}^H$ , in accordance with Needs results in pure silicon.

#### IV. VACANCY AND CONCERTED MECHANISMS

Other point defects, such as vacancies or concerted defects, also contribute to the Ge diffusion in silicon. Mesli and Nylandsted Larsen reported in their paper on irradiated SiGe alloys (see Ref. 25) that pairs made by a germanium atom and a vacancy are stable complexes. According to our calculations, this Ge-vacancy pair has a formation energy equal to  $3.63$  eV, which is greater than that of mixed interstitial defects (see Table II). This value is still lower than a separated Si vacancy and a substitutional germanium (characterized by

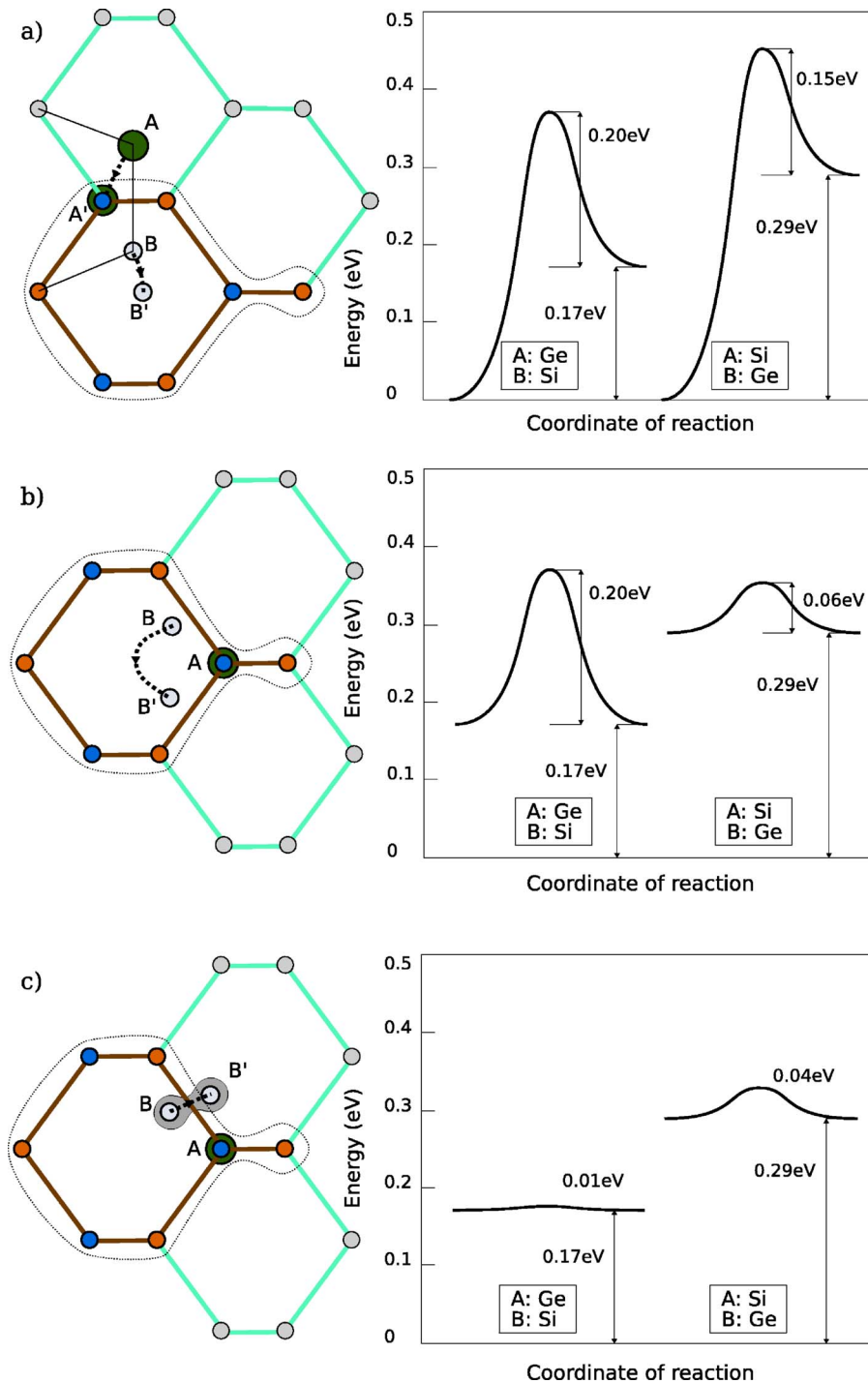


FIG. 2. (Color online) Relative energy variations while one silicon and one germanium move from different interstitial defects. The A (B) sites are occupied either by Si (Ge) or Ge (Si). The energy of the mixed  $D^{110}$  defect is considered as reference energy. Delineated area corresponds to the ten-atom shape and the gray eight-atom shape areas symbolize the energy basins of the *displaced hexagonal* defects. On (a), paths to link  $D^{110}$  defects to hexagonal defects are depicted. On (b), jumps between hexagonal defects of the same pyramid are depicted, and (c) corresponds to movements around the hexagonal position.

$E_f=3.81$  eV). The Ge-vacancy pair is then the most stable configuration, including one germanium and one vacancy. The Ge diffusion mechanism mediated by a vacancy has been extensively studied by Ramanarayanan *et al.*<sup>7</sup> for both high and low (dilute limit) Ge concentrations. It is characterized by  $mn$  movements. The two indices  $m$  and  $n$  denote the relative location of the vacancy and the germanium in terms of nearest-neighbor separation.  $m$  stands for the initial position of the vacancy related to the germanium atom, and  $n$  for the final position. They show that both the exchange Ge-vacancy mechanism (11-movement) and the separation of the Ge-vacancy pair (12-movement followed by a 23-

movement) have to be taken into account to correctly explain the Ge vacancy-assisted diffusion. Indeed, vacancy has to diffuse to a Ge third neighbor to cause net diffusion, and the energy profile of this configuration is equivalent to a dissociated Ge-vacancy pair. Their study consists of an *ab initio* approach of formation and barrier energies coupled to kinetic Monte Carlo (KMC) simulations. Nevertheless, their estimation of energies is limited by the size effect since they used boxes with 64 sites. We have performed the same *ab initio* calculations in 216-site  $2 \times 2 \times 2$  systems (see Fig. 3), which ensures good converged energies as shown by Probert and Payne.<sup>16</sup> It presents quite different barriers, in particular, the

TABLE III. Direct energy paths (in eV) that link the most stable defects in SiGe, calculated in a 216 site  $2 \times 2 \times 2$  system. The given values correspond to the barriers that go from a defect of the first column to a defect of the first row. When the energy is labeled by a star, it denotes defects from different pyramids. The figures in parentheses are the overall barrier (in eV) considering the reference of bulk silicon with one substitutional germanium.

	Mixed $D^{110}$	$Si^H$	$Ge^H$
Mixed $D^{110}$	Not direct	0.37 eV (0.37) <i>dh</i> movement	0.44 eV (0.44) <i>dh</i> movement
$Si^H$	0.20 eV (0.37) <i>dh</i> movement	0.20 eV (0.37) <i>hh</i> movement 0.01 eV* (0.18) <i>b</i> movement	Not direct
$Ge^H$	0.15 eV (0.44) <i>dh</i> movement	Not direct	0.06 eV (0.35) <i>hh</i> movement 0.04 eV* (0.33) <i>b</i> movement

exchange barrier computed in a 216-site  $2 \times 2 \times 2$  system is much higher than in a 64-site  $2 \times 2 \times 2$  system (0.27 eV compared to 0.08 eV). Nevertheless, the shape of the energy profile when the vacancy is moving away from a Ge is conserved. The conclusion, in the dilute limit, about having a capture and/or separation mechanism is then still valid but the effective migration energy will be different, and other KMC simulations, based on our different energetic values, should be done to precisely compute it.

Another possibility of diffusing a germanium throughout the silicon is to use a concerted exchange without any interstitial or vacancy. For this transition, we have studied a SiGe FFCD. Such a defect has already been described in pure silicon by Goedecker *et al.*<sup>13</sup>

The diffusion process (labeled *s* movement) we suggest here switches a substitutional germanium with one of its silicon neighbors. During the switch, the system will transit into

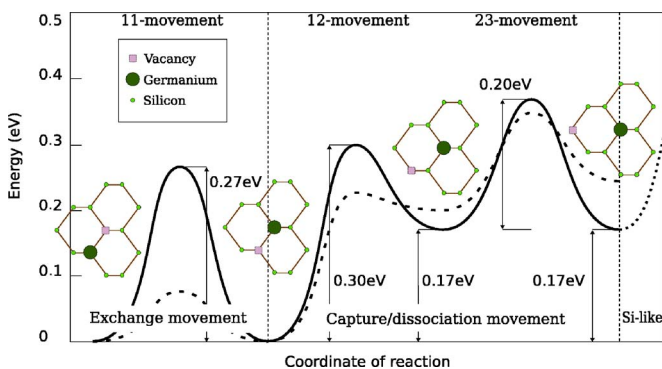


FIG. 3. (Color online) Energy profile during an exchange between a germanium and a vacancy in silicon, followed by a separation movement. All reported energies have been calculated in 216-site  $2 \times 2 \times 2$  systems. The main curve is an interpolation between these points. The dashed curve is taken from the work of Ramanarayanan *et al.* (Ref. 7), resulting from calculations in 64-site  $2 \times 2 \times 2$  systems.

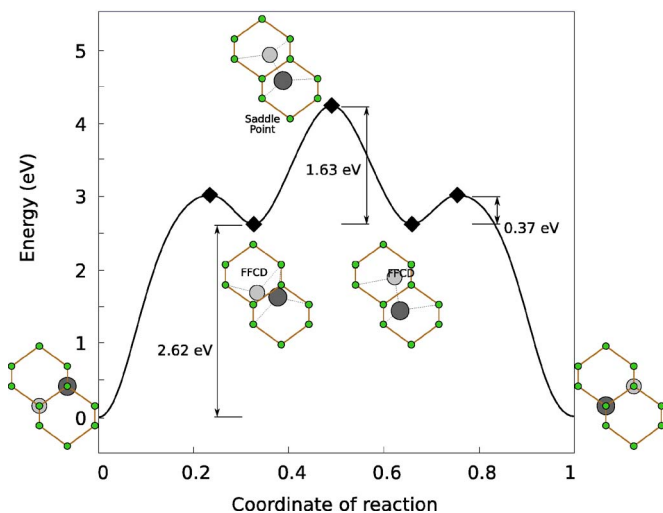


FIG. 4. (Color online) Evolution of the total energy during a switch process between one substitutional silicon and one substitutional germanium. The diamonds represent fully relaxed *ab initio* calculations in boxes of 216 atoms (the line is an interpolation between the calculated energies).

two FFCD. In SiGe it corresponds to a mechanism proposed by Pandey<sup>26</sup> in pure silicon. The main differences here are that intermediate FFCD are stable and that the movement has been fully obtained by NEB calculations without specifying the highest saddle point. The NEB study has been performed in boxes with 64 sites at  $\Gamma$  point and then, saddle points and stable configurations have been checked mostly within better convergence parameters, up to 216-site  $2 \times 2 \times 2$ , with a DIIS algorithm, as well as for the study of the interstitial mechanisms.

The evolution of the energy during the process is detailed in Fig. 4. It is worth noting that the formation energy (2.62 eV) of a mixed FFCD does not differ much from that found in pure silicon ( $E_f=2.59$  eV). The exchange barrier of two FFCD is  $E_m=1.63$  eV. This concerted exchange is then mediated by a low energetic cost defect (the FFCD is only 2.6 eV in SiGe compared to interstitials or vacancies whose formation energies are greater than 3.2 eV) but with a great barrier.

## V. DISCUSSION AND CONCLUSIONS

The three candidate mechanisms for long-distance germanium diffusion in silicon having been presented, we now discuss the contribution of each mechanism, comparing the different energies encountered. In the interstitial and vacancy mechanisms, the diffusion paths are fairly complex with several barriers to be overcome to achieve volume diffusion. The formation energies of these mediators are in the same range, between 3.2 and 3.6 eV, and energies of barriers are quite similar, between 0.2 and 0.4 eV. In these two cases, the diffusion is done with the help of mediators with almost the same high formation cost, but with very low migration energies. We conclude that these two mechanisms are the main participants to diffusion, as observed experimentally by Fahy *et al.*<sup>6</sup>

The effective activation energies ( $E_a = E_f + E_b$ ) of the two mechanisms can be roughly approximated by considering the path with the lowest barrier position that leads to volume diffusion for germanium atoms.

For the vacancy, we find  $E_a \approx 3.63 + 0.37 = 4.00$  eV (see Fig. 3). This predicted value for vacancy diffusion fits well with 4.18 eV, the estimated value<sup>5</sup> for vacancy-mediated diffusion in silicon.

For the interstitial, the migration is believed to take place through a kick-out mechanism.<sup>5</sup> The effective activation energies can then be estimated to be  $E_a \approx 3.25 + 0.44 = 3.69$  eV, with a mixed SiGe dumbbell being the intermediate configuration between hexagonal silicon and hexagonal germanium [see Fig. 2(a)]. To our knowledge, there is no experimental estimation of interstitial diffusion for germanium to compare this value.

As a third mediator of diffusion, the concerted mechanism is quite different from the previous two mediators: once a FFCD is created, the path to the switched position is almost direct. The overall barrier of such a switch is  $E_a = 4.25$  eV. This value is in the same range as that of point-defect mechanisms. The concerted exchange is then a third possible mediator for germanium diffusion. It may be interpreted as the exchange mechanism experimentally reported in the paper of Ural *et al.* (see Refs. 28 and 29).

All these energies are about 1 eV lower than the experimental values ( $\approx 5$  eV) for Ge diffusion in silicon, as reviewed by Fahey *et al.*<sup>6</sup> However, this effective migration energy should derive from a complex combination of Ge diffusion via all mediators and thus a kinetic Monte Carlo simulation is required to precisely simulate the Ge volume diffusion. Indeed, as shown for vacancies in pure silicon,<sup>27</sup>

the experimental activation energies are not always merely linked to the migration energies of individual elementary mechanisms and can even be higher than these energies.

As a conclusion, in this article we have studied three concurrent schemes to explain the germanium diffusion in silicon at low concentrations. The first one requires interstitials. The movement of one germanium is a complex composite scheme based both on dumbbell [110] and on hexagonal defects. The second is assisted by vacancies and requires the separation of the Ge-vacancy pair. These two mechanisms are based on the existence of point defects that have high formation energies, as described in the first part of the article. The third proposed mechanism is based on FFCD. Such defects can easily be created in bulk because of their low formation energy and the fact that neither interstitial nor vacancies are required. Nevertheless, this last mechanism is constrained by its very high migration barrier.

We have quantitatively and extensively shown how these point defects are linked together. We conclude that a qualitative similarity exists between Si and Ge in diffusion processes: the mechanisms are the same but the barriers are different, due to the stabilizing effect of  $D^{110}$  defects. The macroscopic values of activation energies, based on all these detailed elementary mechanisms, have only been estimated and should still be precisely calculated. This should be done with the help of a kinetic Monte Carlo simulation, simulating the diffusion of the three mechanisms in a concurrent way.

#### ACKNOWLEDGMENT

We would like to thank C. Sbraccia for his scripts implementing the NEB method.<sup>19</sup>

- 
- <sup>1</sup>M. L. Lee, E. A. Fitzgerald, M. T. Bulsara, M. T. Currie, and A. Lochtefeld, *J. Appl. Phys.* **97**, 011101 (2005).
- <sup>2</sup>G. L. McVay and A. R. DuCharme, *Phys. Rev. B* **9**, 627 (1974).
- <sup>3</sup>Isolde Collaboration, P. Laitinen, I. Riihimäki, and J. Räisänen, *Phys. Rev. B* **68**, 155209 (2003).
- <sup>4</sup>N. R. Zangenberg, J. Lundsgaard Hansen, J. Fage-Pederson, and A. Nylandsted Larsen, *Phys. Rev. Lett.* **87**, 125901 (2001).
- <sup>5</sup>A. Strohm, T. Voss, W. Frank, P. Laitinen, and J. Räisänen, *Z. Metallkd.* **93**, 737 (2002).
- <sup>6</sup>P. Fahey, S. S. Iyer, and G. J. Scilia, *Appl. Phys. Lett.* **54**, 843 (1989).
- <sup>7</sup>P. Ramanarayanan, K. Cho, and B. M. Clemens, *J. Appl. Phys.* **94**, 174 (2003).
- <sup>8</sup>M. D. Moreira, R. H. Miwa, and P. Venezuela, *Phys. Rev. B* **70**, 115215 (2004).
- <sup>9</sup>L. Wang, P. Clancy, and C. S. Murthy, *Phys. Rev. B* **70**, 165206 (2004).
- <sup>10</sup>W. A. Harrison, *Phys. Rev. B* **57**, 9727 (1998).
- <sup>11</sup>CPMD v3.8.2, copyright IBM Corp. 1990–2001, copyright MPI für Festkörperforschung Stuttgart 1997–2001.
- <sup>12</sup>S. Goedecker, M. Teter, and J. Hutter, *Phys. Rev. B* **54**, 1703 (1996).
- <sup>13</sup>S. Goedecker, T. Deutsch, and L. Billard, *Phys. Rev. Lett.* **88**, 235501 (2002).
- <sup>14</sup>H. J. Monkhorst and J. D. Pack, *Phys. Rev. B* **13**, 5188 (1976).
- <sup>15</sup>O. K. Al-Mushadani and R. J. Needs, *Phys. Rev. B* **68**, 235205 (2003).
- <sup>16</sup>M. I. J. Probert and M. C. Payne, *Phys. Rev. B* **67**, 075204 (2003).
- <sup>17</sup>G. Henkelman, B. P. Uberuaga, and H. Jónsson, *J. Chem. Phys.* **113**, 9901 (2000).
- <sup>18</sup>G. Henkelman and H. Jónsson, *J. Chem. Phys.* **113**, 9978 (2000).
- <sup>19</sup>The up-to-date NEB code can be download. <http://www.sissa.it/sbraccia/gNEB.d/>
- <sup>20</sup>P. Pulay, *Chem. Phys. Lett.* **73**, 393 (1980).
- <sup>21</sup>Y. Bar-Yam and J. D. Joannopoulos, *Phys. Rev. Lett.* **52**, 1129 (1984).
- <sup>22</sup>P. E. Blöchl, E. Smargiassi, R. Car, D. B. Laks, W. Andreoni, and S. T. Pantelides, *Phys. Rev. Lett.* **70**, 2435 (1993).
- <sup>23</sup>R. J. Needs, *J. Phys.: Condens. Matter* **11**, 10437 (1999).
- <sup>24</sup>K. Nishihira and T. Motooka, *Phys. Rev. B* **66**, 233310 (2002).
- <sup>25</sup>A. Mesli and A. Nylandsted Larsen, *Nucl. Instrum. Methods Phys. Res. B* **211**, 80 (2003).
- <sup>26</sup>K. C. Pandey, *Phys. Rev. Lett.* **57**, 2287 (1986).
- <sup>27</sup>D. Caliste and P. Pochet, *Phys. Rev. Lett.* **97**, 135901 (2006).
- <sup>28</sup>A. Ural, P. B. Griffin, and J. D. Plummer, *Appl. Phys. Lett.* **73**, 1706 (1998).
- <sup>29</sup>A. Ural, P. B. Griffin, and J. D. Plummer, *Phys. Rev. Lett.* **83**, 3454 (1999).